CaPdBi: A Nontrivial Topological Candidate

CaPdBi: A Nontrivial Topological Candidate

Sushree Sarita Sahoo[1], Anuroopa Behatha[1], Vishal V Desai[1], V Kanchana[1, a)]

[1]Department of Physics, Institute of Technology Hyderabad, Kandi 502285, Sangareddy, Telangana, India

[a)]Email: kanchana@phy.iith.ac.in

Abstract. In the framework of density functional theory, a comprehensive investigation of the mechanical, dynamical, and electronic properties of the compounds CaPdX (X= Sb and Bi) is performed. The investigated systems are both mechanically and dynamically stable. These compounds are claimed to be metallic by the electronic structure properties, with intriguing crossing points in the close proximity of the Fermi level. With spin orbit coupling (SOC) included, a gap appears at particular crossing points. The predicted electronic band structure shows that the *d*-states of Ca and Pd and the *p*-states of Bi and Sb dominate at the crossing sites. Inversion and time-reversal symmetry, together with the inclusion of SOC, demonstrate that CaPdBi is a Dirac metal. The calculated Z_2 invariants for CaPdSb and CaPdBi are 0 and 1, which infer the trivial and non-trivial strong topological nature, respectively. As a whole, the investigated compound has future scope for its fascinating topological features, one amongst which is the presence of low-energy excitons (Dirac points).

1. Introduction

Topological insulators (TI) have been of increasing interest to the scientific community in recent years because of their extraordinary properties and the potential pathways they enable for future applications. The family of compounds with Bi_2Se_3 which is an archetypal member of the class of compounds belonging to TI [1], are the first ones to have been explored for their thermoelectric applications [2]. They possess two linear dispersive bands that cross the bulk gap, which resulted in the discovery of many Dirac/Weyl metals and semimetals, nodal line semimetals, etc. The band crossings are observed in the bulk as well as surface states in these cases. Under the incorporation of spin orbit coupling (SOC), TaAs turned out to be a Weyl semimetal due to the presence of Weyl points [3]. A few such robust properties were searched for in a huge set of magnetic materials. $Co_3Sn_2S_2$ is one such compound that exhibits the presence of topological surface states and Weyl points connected by Fermi arcs, allowing it to be classified as a topological magnetic semimetal. [4]. Topological materials have promising applications from spintronic devices to energy efficient and non-dissipative devices for quantum computing application. The aspects of Quantum Hall effect and Anomalous Quantum Hall effect in certain materials are also potential applications in terms of Quantum memory and information processing. The Chiral anomaly effect, gravitational anomaly effect, significant intrinsic anomalous Hall and spin Hall effects, and showing a substantial magnetoresistance are only a few of the unusual transport features that topological materials host in bulk [5]. The interesting aspects of topological materials intrigues us in the following direction. In recent years, many Ca-based compounds have been identified to be topological Dirac semimetals [6, 7]. In the present work, the focus is on 111 type Ca based series, CaPdX (X = Sb, Bi) where no

theoretical studies are done so far. The upcoming sections will describe the computational details, and then the results and discussion will be elaborated with a brief conclusion.

2. Computational Details

Using the Vienna Ab-initio Simulation Package (VASP) [8, 9, 10, 11] and the General Gradient approximation- Perdew-Burke-Ernzerhof (GGA-PBE) [12, 13] approximation, the full geometry optimization for the investigated compounds is carried out, and the results are found to be in fair agreement with the experimental parameters [14]. Self-consistency is achieved by the convergence of energy and force up to the orders of 10^{-6} eV and 10^{-2} eV/ Å, respectively. The plane-wave basis sets are created using a 10 × 10 × 5 k-mesh using Monkhorst-pack scheme [15]. The tetrahedron approach has been used to integrate the Brillouin zone. All computations were carried out with a plane-wave energy cut-off of 500 eV. Calculations for the elastic tensor were performed using VASP and a finite difference method. The phonon dispersion computations have chosen to use the density functional perturbation approach, which is implemented in VASP and combined with Phonopy [16]. For ground state energy eigenvalues, the properties of the electronic structure have been calculated.

3. Results and Discussions

The compounds that have been examined, CaPdX (X=Sb, Bi) crystallize in orthorhombic system with the space group *Pnma* (62), with Pd atoms being surrounded tetrahedrally by Sb or Bi atoms respectively. The crystal structure of the compounds along with the irreducible Brillouin zone (IBZ) is represented in the Fig. 1. The GGA-PBE is used for the full geometrical optimization and is found to be consistent with the experimental results. The comparative values of the experimental and optimized results are presented in the Table 1.

Table 1. Details of the experimental and optimized lattice parameters of CaPdX (X = Sb, Bi) within GGA-PBE scheme.

		a (Å)	b (Å)	c (Å)	Volume (Å^3)
CaPdSb	Expt. [14]	7.42	4.75	8.08	285.21
		7.51	4.82	8.22	298.11
CaPdBi	Expt. [14]	7.35	4.61	7.90	268.33
		7.41	4.67	7.99	277.23

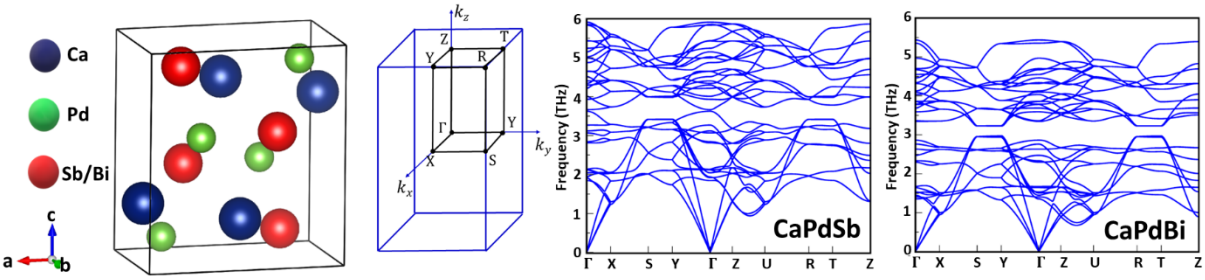

Figure 1. (a-b) Crystal structure details of CaPdX (X = Sb, Bi) along with the irreducible Brillouin zone (IBZ) , (c-d) Computed Phonon dispersion of CaPdX (X = Sb, Bi)

The computation of phonon dispersion establishes the dynamical stability and the phonon band spectrum plotted along high symmetry directions is shown in Fig. 1. The low-frequency modes are formed by the heavier elements, whereas the high-frequency modes by the lighter ones. The gap between low frequency and high frequency optical modes is due to the difference in the atomic

weights of the respective elements in the present compounds. The crystal structure in its reference state exhibits no soft mode for any wave vector and the absence of imaginary phonon modes in the phonon dispersion, confirm the dynamical stability of the compounds.

Proceeding further, the elastic constants for CaPdX (X = Sb, Bi) have been computed which satisfy the Born's stability criteria [17] thus affirming their mechanical stability. The computed elastic constants and properties are tabulated in Table 2. Using these single-crystal elastic constants, the macroscopic elastic moduli such as the bulk (B), shear (G), and Young's modulus (E) with polycrystalline elastic properties are calculated. G_H, as per Hill's average, is the average of shear moduli G_V and G_R calculated using Voigt and Reuss approximation, respectively. The resistance to plastic deformation can be known via the Shear modulus and the ductility or brittleness of the compound can be measured using the Pugh's modulus ratio (B/G). B/G ratio for both the compounds is greater than the critical value of 1.75, indicating the ductile behaviour of the compounds. The ductility is further confirmed by Frantsevich's rule according to which a Poisson's ratio (ν) greater than 0.26 indicates a ductile nature [18].

Table 2. Theoretically obtained elastic constants C_{ij} (GPa), Bulk modulus (B) (GPa), Young's modulus (E) (GPa), Shear modulus (G) (GPa), Poisson's ratio (ν), B/G of CaPdX (X = Sb, Bi)

	C_{11}	C_{22}	C_{33}	C_{12}	C_{13}	C_{23}	C_{44}	C_{55}	C_{66}	B	E	G	ν	B/G
CaPdSb	106.37	146.20	133.10	43.06	51.35	76.33	28.72	41.35	32.70	78.99	89.92	34.31	0.31	2.30
CaPdBi	74.45	102.38	101.62	29.48	37.31	61.64	19.79	24.74	22.34	57.44	60.73	22.94	0.32	2.50

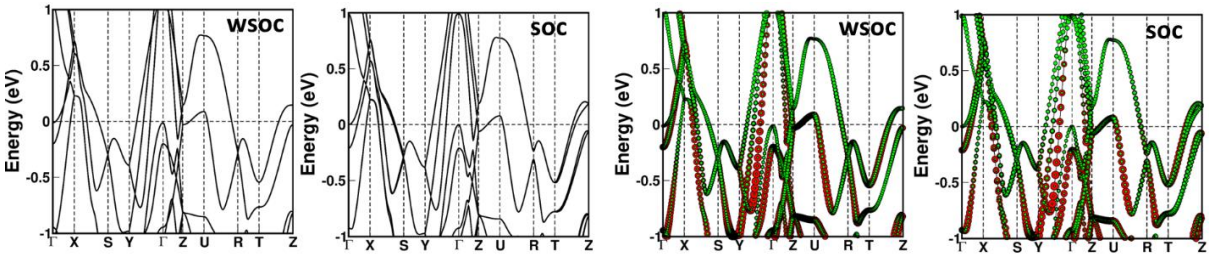

(a) (b) (c) (d)

Figure 2. Electronic band structure of CaPdSb along with the orbital projected bands highlighting the maximum contribution of Pd-*d* (red) and Sb-*p* (green) near the Fermi level (a, c) without the inclusion of spin orbit coupling (WSOC), (b, d) with the inclusion of spin orbit coupling (SOC).

As the next step, the electronic structure properties of these compounds are computed and the same are given in Fig. 2,3. The careful examination of the plots concludes the metallic nature of these systems. Fig. 2 (a) highlights the electronic band structure of CaPdSb. From, Fig. 2 (c, d), it is evident that the states near the Fermi level are predominantly dominated by Pd-*d* and Sb-*p* states. Band crossing points are a typical hallmark of any topological material from a theoretical perspective. A close investigation of the electronic band structure reveals some interesting crossing points in the proximity of the Fermi level along the high symmetry path Γ-X and at the high symmetry points 'S' and 'R' respectively. At these points, we observe the character band mixing of Pd-*d* and Sb-*p* states which provide an insight to analyse the incorporation of spin orbit coupling (SOC). The amalgamation of SOC lifts the degeneracy of the bands. The crossing points are gapped out along Γ-X and at the high symmetry points 'S' and 'R' [Fig. 2 (b, d)].

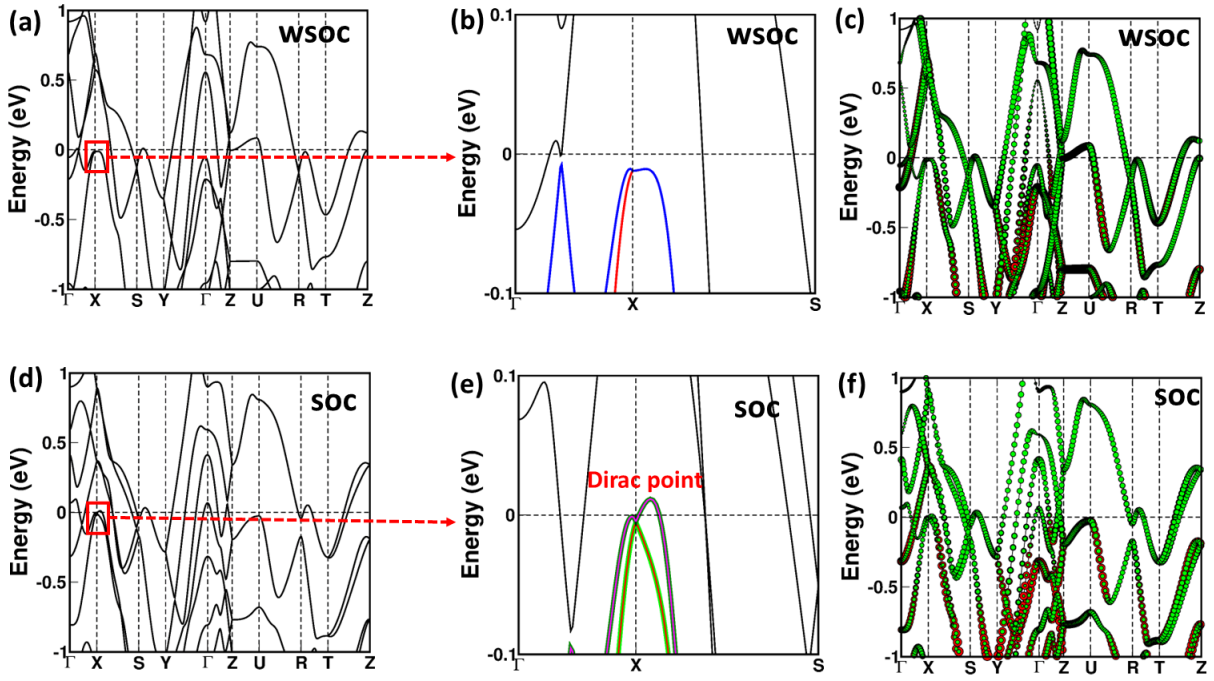

Figure 3. Electronic band structure of CaPdBi along with the orbital projected bands highlighting the maximum contribution of Pd-*d* (red) and Bi-*p* (green) near the Fermi level (a-c) without the inclusion of spin orbit coupling (WSOC), (d-f) with the inclusion of spin orbit coupling (SOC), (b, e) the zoomed-in inset plot of Dirac point at the Fermi level.

The electronic structure properties of CaPdBi without SOC are shown in the Fig. 3 (a-c). One can compare by visualizing the interestingly similar features hosted by CaPdBi and CaPdSb. The presence of 'Bi', the heavier element convinces us to believe that the role of SOC would be more appreciable in CaPdBi and the details can be seen in Fig. 3 (d-f). Nevertheless, we see a separation of the overlapping bands as an effect of SOC along the path X-S which lead us to an intriguing crossing point at X as seen in Fig. 3 (d, e) which is almost at the Fermi level. In addition to lifting the degeneracy of the bands, the inclusion of SOC is responsible for the formation of four-fold degenerate point at the high symmetry point 'X'. This is illustrated in Fig. 3 with a zoomed-in inset [Fig. 3 (b) and (e)] of the Dirac point without and with SOC for CaPdBi, respectively, demonstrating the four-fold band degeneracy with distinct colours. To unearth further topological features of the compound, symmetry analysis is necessary. The investigated systems host inversion symmetry and the absence of magnetic ordering respects the time reversal symmetry too. Preserving both the symmetries along with four-fold degeneracy makes the point observed at 'X' a Dirac point. The Z_2 invariants for both the compounds have been calculated through parity analysis at non-equivalent high symmetry points. Four Z_2 topological invariants $(\nu_0; \nu_1, \nu_2, \nu_3)$, as opposed to a single invariant in two dimensions, are used to define 3D topological insulators. ν_0 is regarded as a strong topological index, whereas the other three are referred to as weak topological indices. The calculated Z_2 values for CaPdSb is found to be (0; 0, 0, 0) whereas CaPdBi shows a value of (1; 0, 0, 0). This evinces the non-trivial strong topological nature of CaPdBi while indicating CaPdSb to be a trivial metal. We expect further prodigious research explorations in this direction because of its non-trivial topological features.

4. Conclusion

The structural, dynamical, mechanical, electronic and topological properties of the compounds CaPdSb and CaPdBi have been extensively investigated using first principles. The phonon dispersion and elastic tensor analysis demonstrate the compounds' dynamical and mechanical stability. They are metals, as evidenced by the electronic structure properties, which also reveal a significant number of intriguing crossing points close to the Fermi-level. The inclusion of SOC brings a number of standout features, such as the opening of the gap at the CaPdBi crossing points, which contributes to the metal's non-trivial topological nature. The contribution to the crossing points is dominated by the *p*-states of Bi or Sb and the *d*-states of Pd. There is ample scope in terms of application in the field of topological materials and thus provides a future scope of research in this field.

5. Acknowledgement

All the authors would like to acknowledge IIT Hyderabad for providing computational facilities. Both Sushree Sarita Sahoo and V Kanchana would like to acknowledge CSIR project with sanction No.(03(1433)/18/EMR-II) for financial support. Anuroopa Behatha would like to acknowledge DST-INSPIRE for fellowship. The authors would also like to acknowledge National Supercomputing Mission (NSM) for providing computing resources of 'PARAM SEVA' at IIT, Hyderabad, which is implemented by C-DAC and supported by the Ministry of Electronics and Information Technology (MeitY) and the Department of Science and Technology (DST), Government of India.

Note: The preliminary results of this work were submitted as an MSc thesis by Vishal V Desai in the IIT Hyderabad Repository [19].

References

[1] Wei Zhang, Rui Yu, Hai-Jun Zhang, Xi Dai, and Zhong Fang. New Journal of Physics, 12(6):065013, (2010).
[2] G. Jeffrey Snyder and Eric S. Toberer. Nature Materials, 7(2):105–114, (2008).
[3] Arnold, F., Shekhar, C., Wu, SC. et al. Nature Communications **7,** 11615 (2016).
[4] Qiunan Xu, Enke Liu, Wujun Shi, Lukas Muechler, Jacob Gayles, Claudia Felser, and Yan Sun. Physical Review B, 97(23):235416, (2018).
[5] Lv, Qianqian, et al. Scientific Reports 11(1), 1-9, (2021).
[6] Nakayama, Kosuke, et al., Physical Review B 102, 041104(R) (2020).
[7] Feng, Liang-Ying, et al., Scientific reports 12(1), 1-8 (2022).
[8] G. Kresse and J. Furthmüller. Computational Materials Science, 6(1):15–50, (1996).
[9] G. Kresse and J. Furthmüller. Physical Review B, 54(16):11169–11186, (1996).
[10] G. Kresse and J. Hafner. Physical Review B, 47(1):558–561, (1993).
[11] G. Kresse and J. Hafner. Physical Review B, 49(20):14251–14269, (1994).
[12] John P. Perdew, Kieron Burke, and Matthias Ernzerhof. Physical Review Letters,77(18):3865–3868, (1996).
[13] John P. Perdew, Kieron Burke, and Matthias Ernzerhof. Physical Review Letters, 78(7):1396–1396, (1997).
[14] Johrendt, D. and Mewis, A. Z. anorg. allg. Chem., 618: 30-34 (1992).
[15] Hendrik J. Monkhorst and James D. Pack. Physical Review B, 13(12):5188–5192, (1976).
[16] Atsushi Togo and Isao Tanaka. Scripta Materialia, 108:1–5, (2015).
[17] Félix Mouhat and François-Xavier Coudert. Physical Review B, 90(22):224104, (2014).
[18] Frantsevich, Ivan Nikitich. "Elastic constants and elastic moduli of metals and insulators." *Reference book* (1982).
[19] Vishal V Desai, *MSc Thesis*, Indian Institute of Technology Hyderabad (2022).